Journal of Molecular Liquids 388 (2023) 122771

Contents lists available at ScienceDirect

Journal of Molecular Liquids

journal homepage: www.elsevier.com/locate/molliq

Evolution of the La(III) ion coordination sphere in ethylammonium nitrate solution upon water addition

Francesco Sessa [a,*], Matteo Busato [a], Cecilia Meneghini [a], Valentina Migliorati [a], Andrea Lapi [a,b], Paola D'Angelo [a,*]

[a] Dipartimento di Chimica, Sapienza Università di Roma, p.le A. Moro 5, 00185, Roma, Italy
[b] Istituto per i Sistemi Biologici (ISB-CNR), Sede Secondaria di Roma-Meccanismi di Reazione, c/o Dipartimento di Chimica, Sapienza Università di Roma, p.le A. Moro 5, 00185, Roma, Italy

ARTICLE INFO

Keywords:
Ethylammonium nitrate
Lanthanides
Ionic liquids
Molecular dynamics
X-ray absorption spectroscopy
Coordination

ABSTRACT

A thorough structural study of $La(NO_3)_3$ salt solutions in mixtures of the ethylammonium nitrate (EAN) ionic liquid (IL) and water with EAN molar fraction (χ_{EAN}) ranging from 0 to 1 has been carried out by means of X-ray absorption spectroscopy (XAS) measurements at the La K-edge and molecular dynamics (MD) simulations. Both the XAS and MD outcomes agree in finding that the composition of the La^{3+} ion first solvation shell undergoes steadily changes when moving from pure water to pure EAN. Upon increasing of the IL concentration, the La^{3+} solvation complexes progressively lose water molecules to accommodate more and more nitrate anions, and the ratio between the two ligands continuously changes across the explored composition range. The nitrate ligands coordinate the metal ion only in a monodentate fashion for the lower EAN contents, while the percentage of bidentate nitrates becomes more and more predominant as the EAN concentration increases. When moving from pure water to pure EAN, the La^{3+} ion coordination passes from a 9-fold tricapped trigonal prismatic geometry to a 12-fold icosahedral one, while a 10-fold coordination with bicapped square antiprism geometry is the dominant species for the mixed compositions. The remarkable flexibility of this solvation complex in accommodating a variable amount of water molecules and nitrate ligands at dependence of the system composition is key for its predominance in all the EAN/water mixtures.

1. Introduction

In recent years, lanthanoid-based compounds have attracted an ever-growing attention from the scientific community due to the sheer number of application fields, ranging from medical diagnostics to organic synthesis, making their solvation chemistry a topic of great interest. [1–3] This holds true especially when the investigated solvents are ionic liquids (ILs), since they offer interesting opportunities for f-elements chemistry. For example, these non-volatile and non-flammable solvents have been explored as media for lanthanoid-mediated reactions, offering a much safer and environmental-friendly alternative to traditional media. [4–13] Moreover, it has been shown that lanthanoid complexes exhibit a much stronger near-infrared photoluminescence in IL solutions than in molecular solvents, with lanthanoid-doped ionogels being new types of luminescent hybrid materials. [14] ILs are also suitable media to carry out ionothermal or microwave-assisted synthesis of lanthanoid coordination compounds or lanthanoid-containing nanoparticles, and ILs featuring lanthanoid-containing anions have shown to be responsive to magnetic fields. [14]

Among the most interesting ILs applications, their employment as extraction media in the nuclear fuel cycle certainly deserves a great attention, as they can replace the traditional organic solvents as receiving phase for the recovery of target lanthanoid ions. [14–16] In this context, even if ILs possess many attractive features, their usually high cost and high viscosity, together with the difficulty in obtaining them with the desired purity level, can limit their use in these application fields, in particular on a large-scale level. Nonetheless, the addition of a co-solvent, like water or alcohols, to the IL phase, can help circumventing these issues, besides being a strategy to tune the physicochemical properties of these "designing solvents" to meet specific requirements. [17] Furthermore, since many ILs are highly hygroscopic, water can be present in these media up to the saturation limit during a liquid-liquid extraction process. Reaching and understanding the solvation process of lanthanoid(III) (Ln^{3+}) salts in IL solutions in the presence of wa-

* Corresponding authors.
E-mail addresses: francesco.sessa@uniroma1.it (F. Sessa), p.dangelo@uniroma1.it (P. D'Angelo).

https://doi.org/10.1016/j.molliq.2023.122771
Received 25 May 2023; Received in revised form 10 July 2023; Accepted 4 August 2023
Available online 11 August 2023

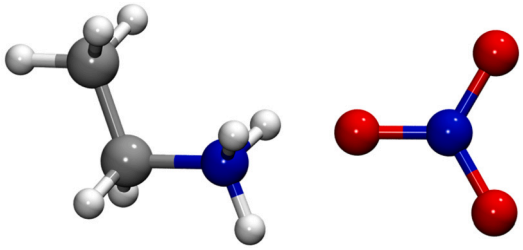

Fig. 1. Molecular structure of EAN. Nitrogen atoms are blue, carbon atoms are grey, oxygen atoms are red and hydrogen atoms are white.

ter therefore becomes an important piece of information to improve the efficiency of extraction procedures for the separation of lanthanoid metals.

In this framework, a great scientific effort has been spent so far to retrieve a clear picture of the solvation properties of Ln^{3+} ions in both aqueous and IL media. [18–22] As far as ILs are concerned, these studies have highlighted a great dependence of the coordination properties in particular upon the nature of the IL anion. [23–29] For example, it has been shown that in the $[C_4mim][PF_6]$ (1-butyl-3-methylimidazolium hexafluorophosphate) IL the first solvation shell of Eu^{3+} ions drastically changes depending on whether the IL was dry or not. [30] Similar results have been reported in a study about the dissolution of $Eu(TfO)_3$ (TfO = trifluoromethanesulfonate) in the $[C_4mim][Tf_2N]$ (1-butyl-3-methylimidazolium bis(trifluoromethylsulfonyl)imide) IL and in the investigation of the coordination properties of uranyl(VI) and plutonil(VI) cations in the $[C_2mim][Tf_2N]$ (1-ethyl-3-methylimidazolium bis(trifluoromethylsulfonyl)imide) IL. [31,32] Even if water, also at low concentrations, dramatically influences the metal ions solvation in ILs featuring weakly coordinating anions, such as PF_6^- or Tf_2N^-, the situation changes for stronger coordinating anions, as in the case of Cl^-. In fact, Eu^{3+} ions in $[C_4mim]Cl$/water mixtures are not coordinated by water molecules if the water molar fraction (χ_{H_2O}) is 0.5 or lower. [33] By raising the χ_{H_2O} above 0.6, water molecules begin entering significantly in the Eu^{3+} solvation complexes, up to the point where, at a χ_{H_2O} of 0.75, water becomes almost the only ligand bound to the Eu^{3+} cations. As a result, it becomes clear that a case-by-case study is required to understand the effect of water concentration on the coordination properties of Ln^{3+} solvation complexes in IL media.

In this work, we employ X-ray absorption spectroscopy (XAS) measurements and molecular dynamics (MD) simulations to investigate the solvation of the La^{3+} ion in mixtures of ethylammonium nitrate (EAN) (Fig. 1) and water. Besides being one of the oldest and most studied ILs, belonging to the protic ionic liquids (PILs) category, EAN has also shown a peculiar behavior when put in contact with water. Indeed, neutron diffraction data have shown that water neither simply dilutes the molecularly dispersed ions of the IL, nor does it just enter the polar region of the pre-existing IL nanostructure. [34] Instead, water molecules interact with the charged groups of the IL merging the inherent structures of the two solvents into a related, but different, nanostructure. Therefore, it is interesting to understand if such structural changes in the solvent are reflected by changes in the solvation complexes of the La^{3+} ions. Moreover, large-scale nuclear fuel reprocessing procedures usually involve the use of concentrated nitric acid, hence Ln^{3+}-nitrate complexes are commonly found as the main lanthanoid-containing species in such applications. [32] Despite having a clear picture of lanthanoid solvation properties in both aqueous and EAN media, our knowledge is lacking on the interplay between water and EAN when acting as cosolvents in a mixed medium. For these reasons, we decided to study $La(NO_3)_3$ solutions in EAN/water mixtures covering the full composition range of the IL and of the cosolvent, *i.e.*, for EAN molar fractions (χ_{EAN}) ranging from 0 to 1. When dealing with the local structure of coordination complexes, the XAS technique is usually the experimental probe of choice due to its selectivity and sensitivity towards the closest environment of the photoabsorber. [35] However, the interpretation of the XAS data is not a trivial task when disordered systems are treated, and previous papers have shown that the XAS technique is particularly effective when aided by the structural information derived from MD simulations. [36–38] Here, our MD/XAS joint approach allowed us to shed light into the peculiar coordination of the La^{3+} ion in EAN/water mixtures and to unravel the changes of the metal ion solvation shell taking place when the mixture composition is varied from pure EAN to pure water. The considerations reported here have implications in several application fields involving lanthanoid metals and ILs as advanced processing media.

2. Materials and methods

2.1. X-ray absorption measurements

EAN was purchased from Iolitec GmbH with a stated purity of > 99%, while $La(NO_3)_3{\cdot}6H_2O$ was purchased from Aldrich with a stated purity of > 99%, and further purification was not carried out. The salt was dried under Argon flux at 200 °C for 2 h to remove water, as previously reported. [39] 0.1 M $La(NO_3)_3$ solutions in water and in EAN were made by adding a stoichiometric amount of the metal salt to freshly distilled water and to the IL, respectively. The EAN solution was sonicated under nitrogen atmosphere for 10 min and then kept under vacuum at 80 °C for 24 h to remove water, and a final water content of 150 ppm was determined by Karl-Fischer titration. The EAN/water mixtures were prepared by mixing stoichiometric amounts of EAN and water to obtain five mixtures with χ_{EAN} = 0.1, 0.2, 0.4, 0.6, and 0.8. A stoichiometric amount of the metal salt was then added to the prepared mixtures to obtain 0.1 M $La(NO_3)_3$ solutions.

La K-edge XAS spectra were collected at room temperature at the BM23 beamline of the European Synchrotron Radiation Facility (ESRF) in transmission geometry. The spectra were collected by using a Si(311) double-crystal monochromator with the second crystal detuned by 20% for harmonic rejection. For each solution at least two spectra were collected and averaged. During the acquisition the samples were kept in a cell with Kapton film windows and Teflon spacers of 2 mm. The XAS spectra were processed by subtracting the smooth pre-edge background fitted with a straight line by using the ATHENA code. [40] The spectra were then normalized at the unit absorption at 300 eV above each edge, where the EXAFS oscillations are small enough to be negligible. The EXAFS spectra have been extracted with a three-segmented cubic spline and the corresponding Fourier transforms (FT) were calculated on the k^2-weighted $\chi(k)k^2$ function in the interval 2.5-10.5 $Å^{-1}$ with no phase shift correction applied.

2.2. MD simulation details

MD simulations of 0.1 M solutions of the $La(NO_3)_3$ salt in EAN/water mixtures were carried out at different χ_{EAN} values ranging from 0 to 1. The composition and size of the simulated systems were chosen to reproduce the experimental densities of the mixtures. Details about the systems are listed in Table S1 of the Supporting Information (SI). As concerns the force field parameters, water was described by the SPC/E model. For the partial charges of the ethylammonium cation we used the charges from the all-atom version of the Optimized Potential for Liquid Simulations (OPLS-AA) force field, [41] while all of the other parameters for the EAN IL were taken from the force field developed by Canongia Lopes and Padua (CL&P). [42,43] A nominal +3.0 charge was assigned to the La^{3+} cation, while the La-La and La-water interactions were described with the Lennard-Jones (LJ) parameters developed by us in ref. 44,45. The LJ parameters for the interaction between the La^{3+} cation and the nitrate anion were also developed by us in ref. 29 to describe the La^{3+} coordination in EAN solution. Parameters for any other mixed term have been obtained by combination rules using the Lorentz-Berthelot criterion.

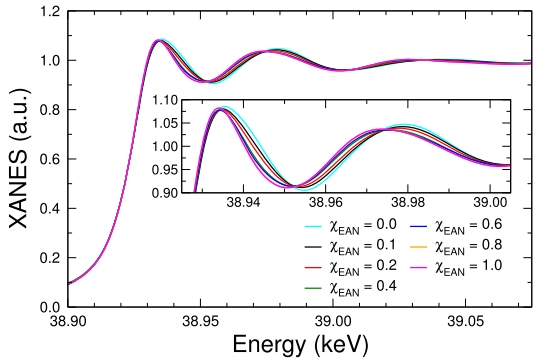

Fig. 2. La K-edge XANES experimental spectra of 0.1 M $La(NO_3)_3$ solutions in EAN/water mixtures at different χ_{EAN} values: 0.0 (cyan), 0.1 (black), 0.2 (red), 0.4 (green), 0.6 (blue), 0.8 (orange), and 1.0 (magenta).

Initial configurations were obtained starting from low density cubic boxes with initial random positions created with the PACKMOL software package, [46] that were compressed in the NPT ensemble until the proper size was reached (see Table S1). The systems were then equilibrated in the NVT ensemble at 300 K for 10 ns, with a final production time of 20 ns for the EAN/water mixtures and of 100 ns for the EAN solution (χ_{EAN} = 1.0). A longer simulation time has been employed for this system because of the slower dynamics typical of ILs, [29] while the diffusion of the species in solution is usually increased when a co-solvent is added to the IL. [10,47] Intermolecular interactions were evaluated explicitly inside a 12 Å cutoff, while electrostatic long-range effects were treated with the Particle Mesh Ewald method. [48] The employed timestep was of 1 fs. The LINCS algorithm [49] was employed to constrain the stretching interactions involving hydrogen atoms. The simulations were performed with the GROMACS package, [50] while the structural analyses were performed by means of in-house written codes. More details about the combined distribution function (CDF) analysis can be found in ref. 51.

3. Results and discussion

3.1. XAS experimental outcomes

Fig. 2 shows the La K-edge XANES (X-ray absorption near edge structure) spectra collected on 0.1 M $La(NO_3)_3$ solutions in EAN/water mixtures with χ_{EAN} = 0.1, 0.2, 0.4, 0.6, and 0.8, together with the experimental data of the $La(NO_3)_3$ salt in aqueous solution and in pure EAN. For sake of comparison, data for the purely aqueous (X_{EAN} = 0.0) and purely EAN (X_{EAN} = 1.0) solutions are reported here from previous works, namely Refs 45 and 29, respectively. Inspection of the spectra reveals a clear decrease of the main oscillation frequency as a function of the water content. Previous works showed that the coordination of the La^{3+} cation is very different between pure water and pure EAN, with the metal ion being coordinated by 9 oxygen atoms in a tricapped trigonal prismatic (TTP) fashion in the former case and by 12 oxygen atoms in an icosahedral geometry in the latter one. [29,45] As the low-energy region of the absorption spectrum is known to be very sensitive to the three-dimensional arrangement of the scattering atoms around the photoabsorber, [36,52–54] the spectral evolution shown in Fig. 2 suggests a gradual change in the solvation complexes formed by the La^{3+} ion in the mixtures going from pure water to pure EAN. To get further insights into this tendency, the EXAFS (extended X-ray absorption fine structure) spectra were extracted from the raw data, and the obtained profiles are reported in Fig. 3. The high energy part of the absorption spectrum is known to have a picometric sensitivity on the first neighbor distances from the photoabsorpber, thus providing a complementary point of view with respect to the XANES one. [35,54] In the EXAFS spectra a shift towards higher frequencies of the main oscillation, which can

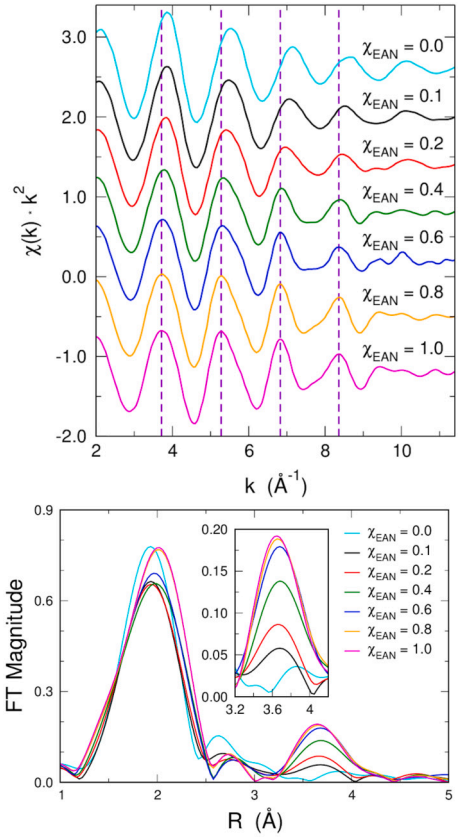

Fig. 3. La K-edge EXAFS spectra (upper panel) and non-phase shift corrected Fourier transforms (lower panel) calculated in the 2.5 - 10.5 $Å^{-1}k$-range of 0.1 M $La(NO_3)_3$ solutions in EAN/water mixtures at different χ_{EAN} values: 0.0 (cyan), 0.1 (black), 0.2 (red), 0.4 (green), 0.6 (blue), 0.8 (orange), and 1.0 (magenta).

reasonably be associated with the La-O first coordination shell, can be observed upon increasing EAN concentration. This outcome evidences the presence of scattering atoms at longer distances from the La^{3+} cation as the EAN content in the mixtures increases. The same scenario can be observed from the FT spectra reported in the lower panel of Fig. 3, where the maximum position of the first peak is found at longer distances for increasing χ_{EAN} values. Another interesting feature of the FT spectra concerns the peak found between ~3.2 and 4 Å, which forms and intensifies as the EAN concentration in the samples rises. Previous studies found that this higher distance peak in the FT's is due to the presence of monodentate nitrate ligands that give rise to La-O-N three-body configurations with a quasi linear intervening angle thus providing strong multiple-scattering contributions. [28,55] Therefore, the increase of this peak intensity suggests that for higher EAN concentrations more and more nitrate anions accommodate in the La^{3+} ion coordination sphere.

3.2. MD results: composition of the La^{3+} ion coordination sphere

To rationalize the XAS experimental findings, we have carried out MD simulations of $La(NO_3)_3$ 0.1 M solutions in EAN/water mixtures with χ_{EAN} = 0.0, 0.1, 0.2, 0.4, 0.6, 0.8, and 1.0, *i.e.*, the same compositions used in the XAS measurements. From the obtained trajectories the La-O_{H_2O} and La-$O_{NO_3^-}$ radial distribution functions $g(r)$'s have been calculated, where O is the oxygen atom of the water molecules and of the nitrate anions, respectively. The obtained curves are shown in Fig. 4, while the corresponding structural parameters are listed in Table 1. The La-O $g(r)$'s show a well defined first peak followed by a depletion zone for both the water and nitrate ligands in all the simulated systems, in-

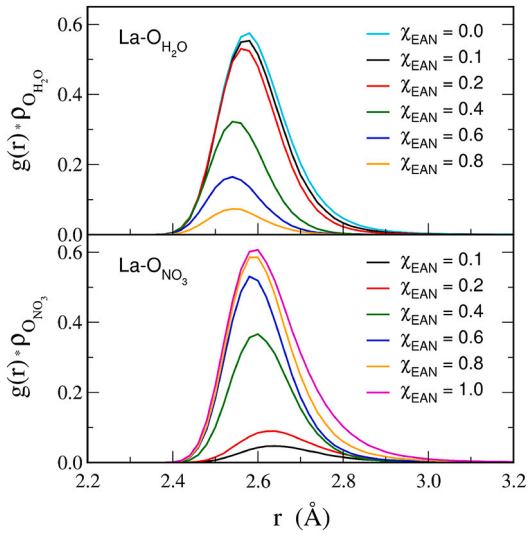

Fig. 4. La-O (upper panel) and La-N (lower panel) radial distribution functions, where O is the oxygen atom of the water molecules and of the nitrate anions, respectively, multiplied by the numerical density of the observed atoms, $g(r)\rho$'s, calculated from the MD simulations of 0.1 M $La(NO_3)_3$ solutions in EAN/water mixtures at different χ_{EAN} values: 0.0 (cyan), 0.1 (black), 0.2 (red), 0.4 (green), 0.6 (blue), 0.8 (orange), and 1.0 (magenta).

Table 1
Structural parameters calculated from the MD simulations of 0.1 M $La(NO_3)_3$ solutions in EAN/water mixtures at different χ_{EAN} values. R_{max} is the position of the $g(r)$ first peak, while CN is the coordination number calculated for the La-O_{H_2O} and La-$O_{NO_3^-}$ distributions using a cutoff value of 3.40 Å. R_{max} and CN are reported also for the first (bi) and second (mono) peak of the La-$N_{NO_3^-}$ $g(r)$'s, where N is the nitrogen atom of nitrate anions. The cutoff values used to calculate the CN for mono- and bidentate coordination are 4.25 and 3.40 Å, respectively.

χ_{EAN} =	0.0	0.1	0.2	0.4	0.6	0.8	1.0
La-O_{H_2O}							
R_{max}	2.57	2.57	2.57	2.55	2.54	2.54	-
CN	9.5	8.8	8.1	4.3	2.2	1.0	-
La-O_{NO_3}							
R_{max}	-	2.64	2.63	2.60	2.59	2.59	2.60
CN	-	1.0	1.8	5.7	8.1	9.7	11.3
La-$N^{(bi)}_{NO_3}$							
R_{max}	-	-	-	-	3.15	3.13	3.11
CN	-	-	-	-	0.3	0.8	2.6
La-$N^{(mono)}_{NO_3}$							
R_{max}	-	3.79	3.77	3.74	3.73	3.74	3.74
CN	-	1.0	1.8	5.7	7.5	8.1	6.1

dicating the presence of a well defined first solvation shell around the metal ion (Fig. 4). In addition, both the La-O_{H_2O} and La-$O_{NO_3^-}$ distributions show marked differences across the whole series. In particular, the intensity of the La-$O_{NO_3^-}$ $g(r)$ first peak is found to increase for higher χ_{EAN} values, while the La-O_{H_2O} distribution becomes less and less intense. The same trend is reflected by the coordination number (CN) values, calculated by integration of the corresponding $g(r)$'s up to a cutoff distance of 3.40 Å (Table 1). The variation of the obtained CNs has been reported also as a function of χ_{EAN} in Fig. 5. The La-O_{H_2O} CN significantly decreases with increasing EAN content, while a simultaneous increase of the La-$O_{NO_3^-}$ one is observed. This trend evidences that the La^{3+} ion first solvation shell progressively loses water molecules to accommodate more and more nitrate ligands as the EAN concentration increases. This result is in agreement with the XAS experimental outcomes, in particular with the rise of the second peak in the FT's spectra for increasing χ_{EAN} values (lower panel of Fig. 3). The total La-O CN

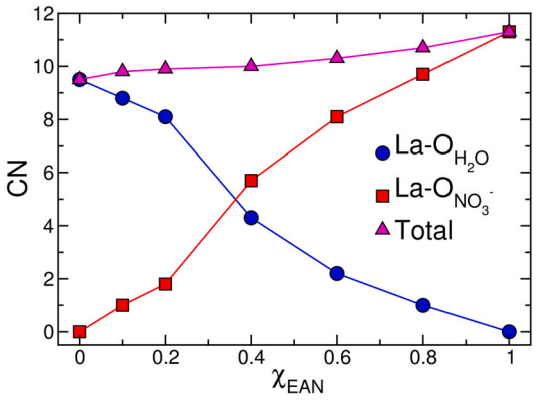

Fig. 5. La-O_{H_2O} (blue circles), La-$O_{NO_3^-}$ (red squares), and La-O_{H_2O} + La-$O_{NO_3^-}$ (magenta triangles) first shell CNs calculated from the MD simulations of 0.1 M $La(NO_3)_3$ solutions in EAN/water mixtures at different χ_{EAN} values. Lines are inserted as a guide to the eye.

obtained from the MD simulations, taking into account both water and nitrate first shell ligands, gradually increases along with χ_{EAN}, from 9.5 oxygen atoms in aqueous solution to 11.3 in EAN solution. This result is in agreement with the gradual change in the La^{3+} ion environment in the mixtures as evidenced by the XANES spectra comparison (Fig. 2), and also suggests that, as the role of nitrate ligands in the solvation complexes becomes more dominant, the coordinating oxygen atoms around the La^{3+} ions arrange themselves in more packed structures. Moreover, from the La-O_{H_2O} and La-$O_{NO_3^-}$ $g(r)$'s, clear trends can be observed in the mean La-O coordination distances. In particular, a slight decrease in the maximum position of both the La-O_{H_2O} and La-$O_{NO_3^-}$ distributions is obtained for increasing EAN concentration (Table 1). However, it is worth noting that the nitrate anion is found to coordinate the La^{3+} ion with a La-O distance that is consistently higher than that provided by water coordination (Table 1). The overall effect is therefore an increase in the mean La-O distances upon increasing EAN concentration. This trend is in agreement with the gradual shift towards higher frequencies of the EXAFS spectra across the mixtures and explains the presence of scattering atoms at longer distances around the La^{3+} photoabsorber for higher EAN concentrations (Fig. 3).

3.3. MD results: structural arrangement of the nitrate ligands

When dealing with nitrate anions, an open question concerns their coordination mode, due to their versatility in behaving as both mono- and bidentate ligands. Note that with bidentate we refer to chelating coordination, in which two oxygen atoms of the nitrate anion bind a single La^{3+} ion. A first general picture can be obtained by observing the La-N $g(r)$'s between the La^{3+} ions and the nitrogen atom of the nitrate anions. The calculated curves are shown in Fig. 6, while the corresponding structural parameters are listed in Table 1. The La-N $g(r)$'s show two characteristic features, namely a first peak in the ~3.0 - 3.4 Å region, and a second one at a ~3.4 - 4.0 Å distance from the reference La^{3+} ion. The former contribution can be associated with nitrogen atoms belonging to bidentate nitrate ligands, and is found only for $\chi_{EAN} >$ 0.5. Instead, the latter feature is due to nitrogen atoms belonging to nitrate anions coordinating in a monodentate fashion. This contribution is present in all the systems and increases in intensity for increasing χ_{EAN} values in the mixtures. These findings indicate that when water molecules are the main constituents of the La^{3+} coordination sphere, the nitrate anions enter the solvation complex by forming a monodentate coordination. On the other hand, when the La^{3+} solvation sphere is mainly constituted by nitrate anions, the nitrate ligands can coordinate either in mono- or bidentate mode. Note that such a trend is broken when we move from the EAN aqueous mixtures to a pure EAN solution. This is due the fact that between the χ_{EAN} = 0.8 mixture and

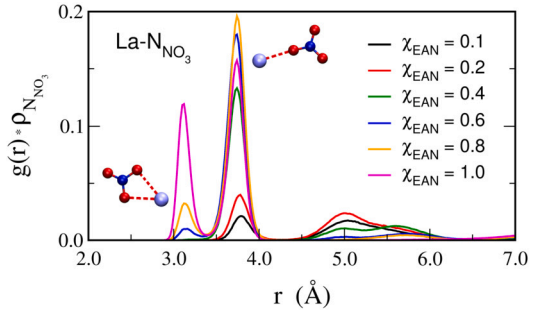

Fig. 6. La-N radial distribution functions multiplied by the numerical density of the observed atoms, $g(r)\rho$'s, where N is the nitrogen atom of the nitrate anions, calculated from the MD simulations of 0.1 M $La(NO_3)_3$ solutions in EAN/water mixtures at different χ_{EAN} values: 0.1 (black), 0.2 (red), 0.4 (green), 0.6 (blue), 0.8 (orange), and 1.0 (magenta).

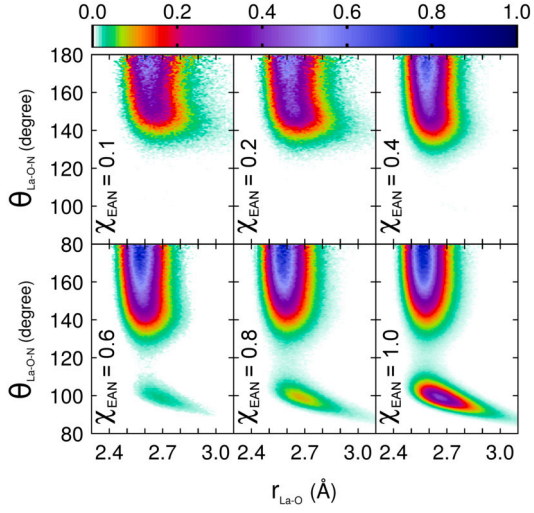

Fig. 7. Combined distribution functions (CDFs) between La-O distances and La-O-N angles, where O and N are the oxygen and nitrogen atoms of the nitrate anion, respectively, calculated from the MD simulations of 0.1 M $La(NO_3)_3$ solutions in EAN/water mixtures at different χ_{EAN} values.

the pure EAN solution there is no increase in the overall number of nitrate ligands in the metal ion first solvation sphere (Table 1), but only a significant change in ratio between monodentate and bidentate coordination modes.

A deeper understanding of the nitrate ligands arrangement can be gained by studying the orientation of the La-O-N angles formed by the coordinating anions with the metal cations. In particular, we evaluated the CDFs between La-O distances and La-O-N angles (Fig. 7), taking into account in the calculation only the oxygen atoms belonging to the La^{3+} coordination shell (*i.e.*, inside a La-N distance shorter than 3.40 Å) and only the La-O-N triplets where the oxygen and nitrogen atoms belong to the same ligand. In the CDFs of all the investigated systems, a broad high probability spot at angles between 150° and 180° is found, which can be connected with nitrate anions coordinating the La^{3+} ion in monodentate fashion. The broad shape of this distribution, especially for systems with $\chi_{EAN} \leq 0.2$, indicates that the monodentate nitrate anions tend to align the O-N vector along the La-O direction forming a nearly linear structure, but this configuration possesses a high configurational freedom and is thus very disordered. Furthermore, for systems with a χ_{EAN} content higher than 0.5, a narrower spot in terms of angular distribution appears at about 100° and progressively intensifies for increasing EAN concentrations. This feature can be associated with bidentate nitrate ligands, which coordinate the La^{3+} ion with two oxygen atoms simultaneously, thus originating a configuration that is more stiff and less free to rotate.

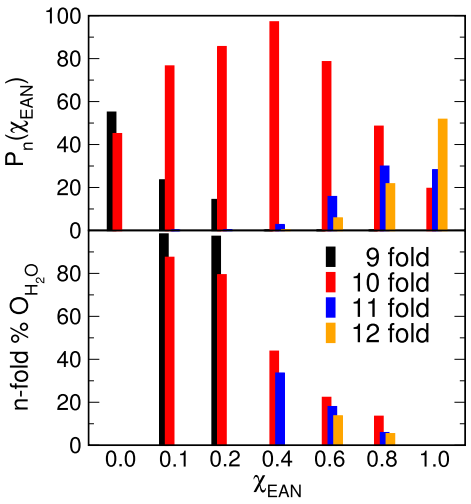

Fig. 8. Coordination number distributions ($P(n)$) for the first shell oxygen atoms of water molecules and nitrate anions (upper panel) and percentage of coordinating oxygen atoms that belong to water ligands (lower panel) calculated from the MD simulations of 0.1 M $La(NO_3)_3$ solutions in EAN/water mixtures at different χ_{EAN} values. Data concerning 9-, 10-, 11- and 12-fold coordination are reported separately in black, red, blue and orange bars, respectively.

3.4. MD simulations: La^{3+} speciation

We have seen that, for higher EAN content in the mixtures, the La^{3+} first solvation shell progressively loses water molecules to accommodate more and more nitrate ligands. Deeper insights into the nature of the solvation complexes formed in the EAN/water mixtures can be obtained by observing the instantaneous coordination number n, defined as the number of atoms of a certain type inside a defined distance from the La^{3+} center. To this aim, we performed this statistical analysis on the La-O coordination number distribution in the mixtures with a cut-off distance of 3.40 Å, and the results are shown in the upper panel of Fig. 8. Although four La-O coordinations can be found throughout the whole series of mixture compositions, ranging from 9 to 12 at dependence of the water content, the dominant species in aqueous solution is the 9-fold one, while in pure EAN it is a 12-fold one, in agreement with the previous findings pointing out a TTP and icosahedral La^{3+} coordination in these two media, respectively. [29,45] However, a different situation can be observed for the EAN/water mixtures. Indeed, the dominant species in the solutions that see the presence of both water and EAN is a complex were the La^{3+} ion is coordinated in a 10-fold fashion. As concerns the other species, 9-fold complexes are found only in mixtures with a water content above 80% ($\chi_{EAN} \leq 0.2$), while 11- and 12-fold complexes are formed in a significant percentage (> 5%) only when the water content falls below 50% ($\chi_{EAN} > 0.5$). For a more thorough analysis of these species, we also evaluated the percentage of coordinating oxygen atoms that belong to water ligands for each kind of complex separately. The results, reported in the lower panel of Fig. 8, show that complexes with a lower number of coordinating oxygen atoms present a systematically higher water content throughout the whole series of mixture compositions. This indicates that water ligands have a stronger affinity towards less packed structures, especially the 9-fold ones, while nitrate ligands prefer the more packed ones. The balance between these two competing affinities in solution can be therefore considered the driving force of the steady structural changes throughout the whole composition range. Interestingly, these opposite trends seem to find their best accommodation in the 10-fold structure, making this complex the dominant species in solution inside the studied range of mixture compositions.

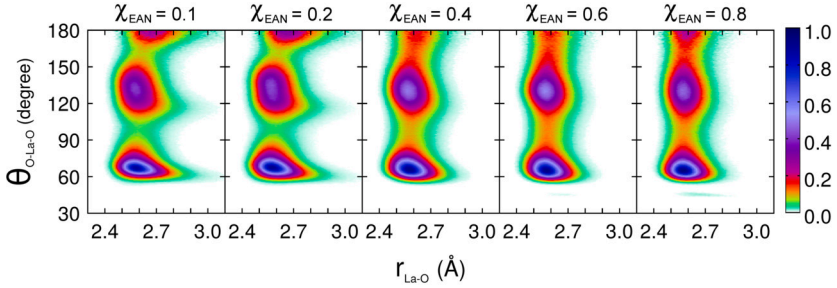

Fig. 9. Combined distribution functions (CDFs) between La-O distances and O-La-O angles calculated for the 10-fold coordination only from the MD simulations of 0.1 M $La(NO_3)_3$ solutions in EAN/water mixtures at different χ_{EAN} values. The calculation included only oxygen atoms inside a 3.40 Å cutoff distance.

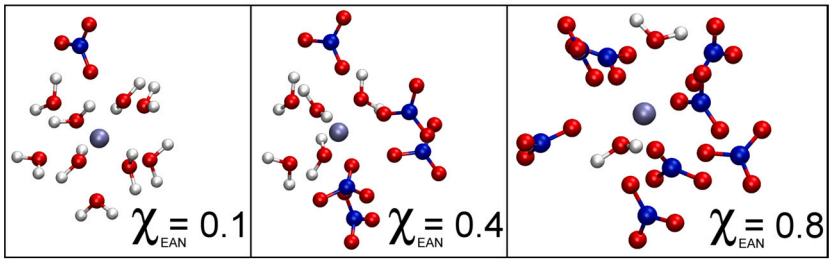

Fig. 10. Representative MD snapshots of the La^{3+} 10-fold solvation complexes extracted from the MD simulations of 0.1 M $La(NO_3)_3$ solutions in EAN/water mixtures with different χ_{EAN} values: 0.1, 0.4, 0.8.

To identify the global geometry of the coordination polyhedra formed by the La^{3+} ion in the EAN/water mixtures, we carried out CDF calculations between La-O distances and O-La-O angles, where O is the oxygen atom of either water molecules or nitrate anions belonging to the coordination sphere of the La^{3+} ion. In order to understand the structure of each solvation complex, we have resorted to perform this analysis separately for the 9-, 10-, 11-, and 12-fold structures and by considering all of the oxygen atoms at a distance from the La^{3+} center shorter than 3.40 Å. The CDFs obtained for the 10-fold coordination, which has turned out to be the dominant one in the EAN/water mixtures, is shown in Fig. 9. Three high probability spots can be observed for all the simulated mixtures peaking at about 65, 130, and 180°. Integration of such features provides similar results in all the studied systems, namely 24, 20 and 1 angles, respectively. Since the 180° feature does not integrate to a number of O-La-O angles equal to half the vertexes of the complex (*i.e.*, 5 angles), it can be deduced that the structure is non-centrosymmetric. Among possible 10-fold non-centrosymmetric geometries, the structural information obtained by the CDFs suggest that it is a bicapped square antiprism (BSAP). Furthermore, although the 10-fold complexes in the different mixtures share a similar geometry, it should be noted that the obtained probability spots display some significant differences, in particular a broader angular distribution for lower EAN concentrations. This indicates that a higher water content in the metal ion coordination sphere is able to induce larger distortions in the solvation complex structure. This high flexibility of the 10-fold complex, which improves its adaptability to different levels of water content, could be the reason why this species is the dominant one in solution when both water and nitrate ligands are involved in the solvation of La^{3+} cations. The MD snapshots shown in Fig. 10 provide a pictorial example of the 10-fold La^{3+} solvation complexes for different χ_{EAN} values.

As concerns the CDFs calculated, it should be stressed that the presence of coordinations other than the 10-fold one is not significant in all mixtures. Therefore, the CDFs for a given complex have been calculated only for those systems were it is found at least 5% of the time. The functions obtained for the 9-fold complexes, reported in Figure S1, are very similar to those already found in previous works on La^{3+} ion coordination in aqueous solution, and are the typical fingerprint of the TTP coordination. [44,45] As concerns the CDFs for the 12-fold complexes (Figure S2), they show three peaks at 65, 120 and 180°, which are compatible with the previously determined icosahedral nitrato-complex formed by the La^{3+} ion in EAN solution. [28,29] As concerns the 11-fold complexes, they also display three well defined peaks at 65, 120 and 180° (Figure S3), which are very similar to the ones obtained for the icosahedral 12-fold geometry (Figure S2), albeit broader and thus more distorted. Integration of the high probability spots results in a number of 27, 25 and 3 angles, respectively, which is consistent with an edge-contracted icosahedral structure, *i.e.*, a geometry in which two vertexes of a regular icosahedron are collapsed into one. Such structure could easily form around the La^{3+} cation when a first shell oxygen atom of an icosahedral complex leaves, inducing a rearrangement of the remaining ligands. Reference models of all the structures proposed here are shown in Figure S4.

4. Conclusions

In this work, we have studied the structural properties of $La(NO_3)_3$ salt solutions in mixtures of EAN and water by means of XAS measurements and MD simulations, with the aim of achieving a reliable atomistic description of the La^{3+} ion coordination through the whole composition range with χ_{EAN} going from 0 to 1. A steadily change in the local environment around the La^{3+} ions is observed from pure water to pure EAN, where the metal ion first solvation shell progressively loses water molecules to accommodate more and more nitrate anions as the EAN concentration increases. Both water and nitrate ligands populate the La^{3+} ion coordination complexes in all the EAN/water mixtures. In this way, even when nitrate anions are present in great excess (*i.e.*, for $\chi_{EAN} = 0.8$), they never saturate the metal ion first solvation sphere, which still contains water molecules. A different behavior of the IL anions is observed depending upon the EAN concentration, with nitrate ligands coordinating the La^{3+} ions in a monodentate fashion for low EAN contents, while the percentage of bidentate coordination becomes more and more significant as the EAN concentration increases. The orientation of the monodentate-binding nitrates is very disordered and possesses a great orientational freedom, while a more ordered arrangement has been detected for the bidentate ones.

Going from pure water to pure EAN, the total first-shell coordination number of the La^{3+} ions ($La\text{-}O_{H_2O} + La\text{-}O_{NO_3^-}$) increases of about

three units, going from a 9-fold complex with TTP geometry in aqueous solution to a 12-fold icosahedral nitrato-complex in pure EAN, in agreement with previous determinations. [29,45] This indicates that the coordinating water molecules have a stronger affinity towards less packed structures, while nitrate ligands prefer the more packed ones. In the EAN/water mixtures these two opposite trends find their accommodation in a 10-fold coordination with BSAP geometry, which is the dominant species for all the mixed compositions. The structure of this solvation complex shows a remarkable flexibility, which allows it to adapt to the changes in the ligand-ligand interactions that comes from different levels of water content in the media.

The gradual change that we observed in the La^{3+} ions coordination going from pure water to pure EAN is at variance with what was found for other Ln^{3+} ions in aqueous mixtures of ILs featuring other anions, either with strong (*e.g.*, Cl^-) or weak (*e.g.*, Tf_2N^-, TfO^- or PF_6^-) coordinating abilities. In fact, in those cases the changes in the population of the metal first solvation sphere were found to be confined in a narrow range of the mixture compositions, with either only water or the IL anions coordinating the lanthanoid ions outside that range. [30–33] Instead, the speciation and structure of the La^{3+}-nitrato complexes have proven to change throughout the whole range of composition in the inspected EAN/water mixtures and to strongly depend on the water content of the media. Thus, a correct monitoring of the water content can be critical in any application that involves nitrato complexes of lanthanoid metals.

CRediT authorship contribution statement

Francesco Sessa: Data curation, Writing – original draft. **Matteo Busato:** Data curation, Investigation, Writing – original draft. **Cecilia Meneghini:** Data curation, Software. **Valentina Migliorati:** Data curation, Writing – original draft. **Andrea Lapi:** Data curation. **Paola D'Angelo:** Conceptualization, Methodology, Writing – review & editing.

Declaration of competing interest

The authors declare that they have no known competing financial interests or personal relationships that could have appeared to influence the work reported in this paper.

Data availability

Data will be made available on request.

Acknowledgements

This work was supported by the University of Rome "La Sapienza" (Progetti Ateneo 2015 n. C26N159PNB and n. C26H159F5B) and by the CINECA supercomputing centers through the grant IscrC_LABILE.

Appendix A. Supplementary material

Supplementary material related to this article can be found online at https://doi.org/10.1016/j.molliq.2023.122771.

References

[1] S.V. Eliseeva, J.-C.G. Bunzli, Lanthanide luminescence for functional materials and bio-sciences, Chem. Soc. Rev. 39 (2010) 189–227.
[2] H. Dong, S.-R. Du, X.-Y. Zheng, G.-M. Lyu, L.-D. Sun, L.-D. Li, P.-Z. Zhang, C. Zhang, C.-H. Yan, Lanthanide nanoparticles: from design toward bioimaging and therapy, Chem. Rev. 115 (2015) 10725–10815.
[3] R.D. Teo, J. Termini, H.B. Gray, Lanthanides: applications in cancer diagnosis and therapy, J. Med. Chem. 59 (2016) 6012–6024.
[4] I. Billard, A. Ouadi, C. Gaillard, Liquid–liquid extraction of actinides, lanthanides, and fission products by use of ionic liquids: from discovery to understanding, Anal. Bioanal. Chem. 400 (2011) 1555–1566.
[5] V. Migliorati, P. Ballirano, L. Gontrani, S. Materazzi, F. Ceccacci, R. Caminiti, A combined theoretical and experimental study of solid octyl and decylammonium chlorides and of their aqueous solutions, J. Phys. Chem. B 117 (2013) 7806–7818.
[6] R. Rogers, K. Seddon (Eds.), Ionic Liquids IIIB: Fundamentals, Progress, Challenges, and Opportunities: Transformations and Processes, ACS Symp. Ser., vol. 902, American Chemical Society, Washington D.C., 2005.
[7] A. Serva, V. Migliorati, A. Lapi, G. Aquilanti, A. Arcovito, P. D'Angelo, Structural properties of geminal dicationic ionic liquid/water mixtures: a theoretical and experimental insight, Phys. Chem. Chem. Phys. 18 (2016) 16544–16554.
[8] P. D'Angelo, A. Serva, G. Aquilanti, S. Pascarelli, V. Migliorati, Structural properties and aggregation behavior of 1-hexyl-3-methylimidazolium iodide in aqueous solutions, J. Phys. Chem. B 119 (2015) 14515–14526.
[9] V. Migliorati, A. Serva, G. Aquilanti, S. Pascarelli, P. D'Angelo, Local order and long range correlations in imidazolium halide ionic liquids: a combined molecular dynamics and XAS study, Phys. Chem. Chem. Phys. 17 (2015) 16443–16453.
[10] V. Migliorati, A. Zitolo, P. D'Angelo, Using a combined theoretical and experimental approach to understand the structure and dynamics of imidazolium based ionic liquids/water mixtures. 1. MD simulations, J. Phys. Chem. B 117 (2013) 12505–12515.
[11] P. D'Angelo, A. Zitolo, G. Aquilanti, V. Migliorati, Using a combined theoretical and experimental approach to understand the structure and dynamics of imidazolium-based ionic liquids/water mixtures. 2. Exafs spectroscopy, J. Phys. Chem. B 117 (41) (2013) 12516–12524.
[12] V. Migliorati, A. Serva, G. Aquilanti, L. Olivi, S. Pascarelli, O. Mathon, P. D'Angelo, Combining EXAFS spectroscopy and molecular dynamics simulations to understand the structural and dynamic properties of an imidazolium iodide ionic liquid, Phys. Chem. Chem. Phys. 17 (2015) 2464–2474.
[13] V. Migliorati, P. Ballirano, L. Gontrani, R. Caminiti, Crystal polymorphism of hexylammonium chloride and structural properties of its mixtures with water, J. Phys. Chem. B 116 (2012) 2104–2113.
[14] K. Binnemans, Lanthanides and actinides in ionic liquids, Chem. Rev. 107 (2007) 2592–2614.
[15] S.A. Ansari, L. Liu, P.D. Dau, J.K. Gibson, L. Rao, Unusual complexation of nitrate with lanthanides in a wet ionic liquid: a new approach for aqueous separation of trivalent f-elements using an ionic liquid as solvent, RSC Adv. 4 (2014) 37988–37991.
[16] S.A. Ansari, L. Liu, L. Rao, Binary lanthanide(III)/nitrate and ternary lanthanide(III)/nitrate/chloride complexes in an ionic liquid containing water: optical absorption and luminescence studies, Dalton Trans. 44 (2015) 2907–2914.
[17] M. Llaver, E.F. Fiorentini, P.Y. Quintas, M.N. Oviedo, M.B. Botella Arenas, R.G. Wuilloud, Task-specific ionic liquids: applications in sample preparation and the chemistry behind their selectivity, Adv. Sample Prep. 1 (2022) 100004.
[18] P. D'Angelo, A. Zitolo, V. Migliorati, G. Chillemi, M. Duvail, P. Vitorge, S. Abadie, R. Spezia, Revised ionic radii of lanthanoid(III) ions in aqueous solution, Inorg. Chem. 50 (2011) 4572–4579.
[19] P. D'Angelo, R. Spezia, Hydration of lanthanoids(III) and actinoids(III): an experimental/theoretical saga, Chem. Eur. J. 18 (2012) 11162–11178.
[20] I. Persson, P. D'Angelo, S. De Panfilis, M. Sandstrom, L. Eriksson, Hydration of lanthanoid(III) ions in aqueous solution and crystalline hydrates studied by EXAFS spectroscopy and crystallography: the myth of the "gadolinium break", Chem. Eur. J. 14 (2008) 3056–3066.
[21] M. Duvail, P. D'Angelo, M.-P. Gaigeot, P. Vitorge, R. Spezia, What first principles molecular dynamics can tell us about EXAFS spectroscopy of radioactive heavy metal cations in water, Radiochim. Acta 97 (2009) 339–346.
[22] M. Duvail, R. Spezia, P. Vitorge, A dynamic model to explain hydration behaviour along the lanthanide series, ChemPhysChem 9 (2008) 693–696.
[23] M. Lipsztajn, R.A. Osteryoung, Electrochemistry in neutral ambient-temperature ionic liquids. 1. Studies of iron(III), neodymium(III), and lithium(I), Inorg. Chem. 24 (1985) 716–719.
[24] A. Chaumont, G. Wipff, Solvation of M^{3+} lanthanide cations in room-temperature ionic liquids. A molecular dynamics investigation, Phys. Chem. Chem. Phys. 5 (2003) 3481–3488.
[25] A. Chaumont, G. Wipff, Solvation of uranyl(II), europium(III) and europium(II) cations in "basic" room-temperature ionic liquids: a theoretical study, Chem. Eur. J. 10 (2004) 3919–3930.
[26] A. Chaumont, G. Wipff, Solvation of ln(III) lanthanide cations in the [BMI][SCN], $[MeBu_3N][SCN]$, and $[BMI]_5[Ln(NCS)_8]$ ionic liquids: a molecular dynamics study, Inorg. Chem. 48 (2009) 4277–4289.
[27] M. Duvail, P. Guilbaud, Understanding the nitrate coordination to Eu^{3+} ions in solution by potential of mean force calculations, Phys. Chem. Chem. Phys. 13 (2011) 5840–5847.
[28] A. Serva, V. Migliorati, R. Spezia, P. D'Angelo, How does Ce^{III} nitrate dissolve in a protic ionic liquid? A combined molecular dynamics and EXAFS study, Chem. Eur. J. 23 (2017) 8424–8433.
[29] F. Sessa, V. Migliorati, A. Lapi, P. D'Angelo, Ce^{3+} and La^{3+} ions in ethylammonium nitrate: a XANES and molecular dynamics investigation, Chem. Phys. Lett. 706 (2018) 311–316.
[30] A. Chaumont, G. Wipff, Solvation of uranyl(II) and europium(III) cations and their chloro complexes in a room-temperature ionic liquid. A theoretical study of the effect of solvent "humidity", Inorg. Chem. 43 (2004) 5891–5901.

[31] I. Billard, S. Mekki, C. Gaillard, P. Hesemann, G. Moutiers, C. Mariet, A. Labet, J.-C.G. Bünzli, Eu^{III} luminescence in a hygroscopic ionic liquid: effect of water and evidence for a complexation process, Eur. J. Inorg. Chem. 2004 (2004) 1190–1197.
[32] K.A. Maerzke, G.S. Goff, W.H. Runde, W.F. Schneider, E.J. Maginn, Structure and dynamics of uranyl(VI) and plutonyl(VI) cations in ionic liquid/water mixtures via molecular dynamics simulations, J. Phys. Chem. B 117 (2013) 10852–10868.
[33] S. Samikkanu, K. Mellem, M. Berry, P.S. May, Luminescence properties and water coordination of Eu^{3+} in the binary solvent mixture water/1-butyl-3-methylimidazolium chloride, Inorg. Chem. 46 (2007) 7121–7128.
[34] R. Hayes, S. Imberti, G.G. Warr, R. Atkin, How water dissolves in protic ionic liquids, Angew. Chem., Int. Ed. 51 (2012) 7468–7471.
[35] A. Filipponi, P. D'Angelo, XAS in Liquid Systems, John Wiley I& Sons, Ltd, 2016, pp. 745–771, Ch. 25.
[36] P. D'Angelo, V. Migliorati, F. Sessa, G. Mancini, I. Persson, XANES reveals the flexible nature of hydrated strontium in aqueous solution, J. Phys. Chem. B 120 (2016) 4114–4124.
[37] F. Sessa, V. Migliorati, A. Serva, A. Lapi, G. Aquilanti, G. Mancini, P. D'Angelo, On the coordination of Zn^{2+} ion in Tf_2N^- based ionic liquids: structural and dynamic properties depending on the nature of the organic cation, Phys. Chem. Chem. Phys. 20 (2018) 2662–2675.
[38] M. Busato, P. D'Angelo, A. Melchior, Solvation of Zn^{2+} ion in 1-alkyl-3-methylimidazolium bis(trifluoromethylsulfonyl)imide ionic liquids: a molecular dynamics and X-ray absorption study, Phys. Chem. Chem. Phys. 21 (2019) 6958–6969.
[39] S. Mentus, D. Jelić, V. Grudić, Lanthanum nitrate decomposition by both temperature programmed heating and citrate gel combustion - comparative study, J. Therm. Anal. Calorim. 90 (2007) 393–397.
[40] B. Ravel, M. Newville, *ATHENA*, *ARTEMIS*, *HEPHAESTUS*: data analysis for X-ray absorption spectroscopy using *IFEFFIT*, J. Synchrotron Radiat. 12 (2005) 537–541.
[41] W.L. Jorgensen, J.P. Ulmschneider, J. Tirado-Rives, Free energies of hydration from a generalized born model and an all-atom force field, J. Phys. Chem. B 108 (41) (2004) 16264–16270.
[42] J.N. Canongia Lopes, J. Deschamps, A.A.H. Pádua, Modeling ionic liquids using a systematic all-atom force field, J. Phys. Chem. B 108 (2004) 2038–2047.
[43] J.N. Canongia Lopes, A.A.H. Pádua, Molecular force field for ionic liquids III: imidazolium, pyridinium, and phosphonium cations; chloride, bromide, and dicyanamide anions, J. Phys. Chem. B 110 (2006) 19586–19592.
[44] V. Migliorati, A. Serva, F.M. Terenzio, P. D'Angelo, Development of Lennard-Jones and Buckingham potentials for lanthanoid ions in water, Inorg. Chem. 56 (11) (2017) 6214–6224.
[45] V. Migliorati, A. Serva, F. Sessa, A. Lapi, P. D'Angelo, Influence of counterions on the hydration structure of lanthanide ions in dilute aqueous solutions, J. Phys. Chem. B 122 (2018) 2779–2791.
[46] L. Martínez, R. Andrade, E.G. Birgin, J.M. Martínez, Packmol: a package for building initial configurations for molecular dynamics simulations, J. Comput. Chem. 30 (2009) 2157–2164.
[47] V. Migliorati, A. Lapi, P. D'Angelo, Unraveling the solvation geometries of the lanthanum(III) bistriflimide salt in ionic liquid/acetonitrile mixtures, Phys. Chem. Chem. Phys. 22 (2020) 20434–20443.
[48] U. Essmann, L. Perera, M.L. Berkowitz, T. Darden, H. Lee, L.G. Pedersen, A smooth particle mesh Ewald method, J. Chem. Phys. 103 (1995) 8577–8593.
[49] B. Hess, H. Bekker, H.J.C. Berendsen, J.G.E.M. Fraaije, Lincs: a linear constraint solver for molecular simulations, J. Comput. Chem. 18 (1997) 1463–1472.
[50] H.J.C. Berendsen, D. van der Spoel, R. van Drunen, Gromacs: a message-passing parallel molecular dynamics implementation, Comput. Phys. Commun. 91 (1995) 43–56.
[51] F. Sessa, P. D'Angelo, V. Migliorati, Combined distribution functions: a powerful tool to identify cation coordination geometries in liquid systems, Chem. Phys. Lett. 691 (2018) 437–443.
[52] J.L. Fulton, S.M. Heald, Y.S. Badyal, J.M. Simonson, Understanding the effects of concentration on the solvation structure of Ca^{2+} in aqueous solution. I: the perspective on local structure from EXAFS and XANES, J. Phys. Chem. A 107 (2003) 4688–4696.
[53] J. Garcia, M. Benfatto, C. Natoli, A. Bianconi, A. Fontaine, H. Tolentino, The quantitative Jahn-Teller distortion of the Cu^{2+} site in aqueous solution by XANES spectroscopy, Chem. Phys. 132 (1989) 295–302.
[54] P. D'Angelo, M. Benfatto, S. Della Longa, N.V. Pavel, Combined XANES and EXAFS analysis of Co^{2+}, Ni^{2+}, and Zn^{2+} aqueous solutions, Phys. Rev. B 66 (2002) 064209.
[55] L. Liu, G. Tian, L. Rao, Effect of solvation? Complexation of neodymium(III) with nitrate in an ionic liquid ($BumimTf_2N$) in comparison with water, Solvent Extr. Ion Exch. 31 (2013) 384–400.